IEEE Access
Multidisciplinary | Rapid Review | Open Access Journal

Received February 24, 2021, accepted March 12, 2021, date of publication March 17, 2021, date of current version March 23, 2021.

Digital Object Identifier 10.1109/ACCESS.2021.3066237

On Entanglement Assisted Classical Optical Communications

IVAN B. DJORDJEVIC, (Fellow, IEEE)
Department of Electrical and Computer Engineering, The University of Arizona, Tucson AZ 85721, USA
e-mail: ivan@email.arizona.edu

This work was supported in part by NSF.

ABSTRACT Entanglement assisted communication is advocated by numerous authors as an alternative to classical communication offering significant improvement in channel capacity, in particular in noisy regime. In all those papers it is always assumed that entanglement can be distributed without any imperfections, except for attenuation. We demonstrate that under imperfect pre-shared entanglement distribution, assuming that entanglement distribution channel is modeled as a noisy and lossy Bosonic channel, the entanglement assisted communication can be inferior compared to the classical communication, depending on the parameters of the distribution channel. We identify the conditions under which entanglement assistance can still provide an advantage over the classical case. In particular, when both communication and entanglement distribution channels are not used for entanglement assisted communication but rather for classical transmission instead then the classical capacity is always higher than the entanglement assisted capacity. We also study the entanglement assisted communication under the strong atmospheric turbulence effects.

INDEX TERMS Quantum communication, classical communication, entanglement, entanglement assisted capacity, Holevo capacity, shannon capacity.

I. INTRODUCTION

Quantum information processing (QIP) opens new opportunities for high-precision sensing, secure communications, and ultra-high-performance computing [1]–[3]. Entanglement represents a unique resource for QIP enabling new type of sensors with measurement sensitivities beyond the classical limit, allows quantum computers to solve numerically intractable problems, and provides certifiable security for data transmissions whose security is guaranteed fundamental laws of physics as opposed to unproven mathematical assumptions employed in computational security-based cryptography.

The pre-shared entanglement can also be used, at least in theory, to improve the classical communication capacity [4]–[8]. In addition to secure communications and improved sensor sensitivity, the pre-shared entanglement can be used in distributed quantum computing [9], entanglement assisted (EA) distributed sensing [10], and provably-secure quantum computer access [11], to mention few. The EA classical capacity, that is the maximum of quantum mutual information [4], has been known for decades [4]–[6]; however, the structure of optimum quantum receiver, achieving the EA capacity, has not been determined yet. Moreover, in the determination of EA capacity it is assumed that the distribution of pre-shared entanglement is perfect. To distribute the entangled signal-idler photon pairs either the satellite-to-ground links or fiber-based quantum network, as illustrated in Fig. 1, can be used. Unfortunately, the satellite-to-ground link will experience diffraction loss, atmospheric turbulence effects, scattering effects, and background radiation; and clearly the distribution of entanglement cannot be considered as ideal. In similar fashion, in fiber-based quantum network we cannot ignore the dispersion effects, channel attenuation, and phase noise. Moreover, the entangled states need to be stored in quantum memories before being used and given that the quantum memories are imperfect someone has to use quantum error correction to deal with decoherence effects.

In this paper we study EA channel capacity assuming that the entanglement distribution is imperfect, subject to attenuation and noise, and compare it against classical channel capacity for homodyne and heterodyne detections. We demonstrate that in the presence of imperfect pre-shared entanglement, EA assisted capacity get reduced significantly and when signal-idler photon pairs get distributed over the same noisy channel, used for data transmission, EA assisted

The associate editor coordinating the review of this manuscript and approving it for publication was Barbara Masini.

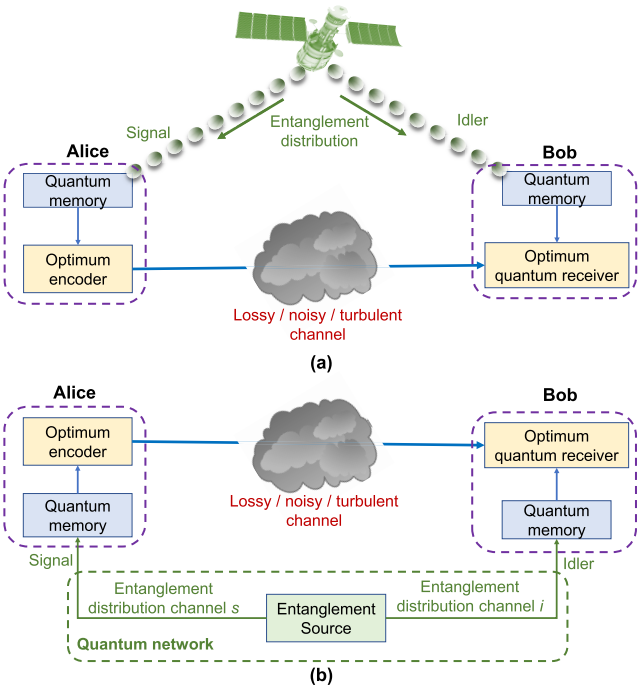

FIGURE 1. Illustrating the entanglement assisted classical optical communication concept: (a) satellite-based entanglement distribution and (b) quantum network-based entanglement distribution.

capacity can be worse than classical capacity with homodyne detection. To achieve the EA capacity it has been shown by Holevo and Werner in [4] that someone needs to use two-mode Gaussian states. We also describe the optimum encoding based on Gaussian modulation of signal photon in two-mode-squeezed-vacuum (TMSV) state. The authors of ref. [8] have shown that EA capacity can also be achieved with random phase modulation. Finally, we study the degradation of EA capacity improvement over classical capacity in the presence of strong atmospheric turbulence effects.

The paper is organized as follows. The realistic entanglement assisted free-space optical (FSO) and fiber-optics communication systems are described in Section II. In Section III, the comparison between EA capacity and classical capacities is performed assuming that entanglement distribution channel is imperfect, modeled as a lossy and noisy Bosonic channel. In Section IV EA communication over FSO links is studied. Concluding remarks are provided in Sec. V.

II. REALISTIC ENTANGLEMENT ASSISTED CLASSICAL OPTICAL COMMUNICATION SYSTEMS

As illustrated in Fig. 1(a), the satellites can be used in entanglement distribution. This is favorable scenario given that satellite-to-ground links are less sensitive to atmospheric turbulence effects compared to ground-to-satellite links. The entangled states are stored in quantum memories and used when needed. Alice employs her signal photon of entangled pair and transmits the classical data, imposed on the signal photon, over lossy, noisy, and possibly turbulent optical channel. On receiver side, Bob employs the entangled idler photon to decide on what was transmitted on signal photon

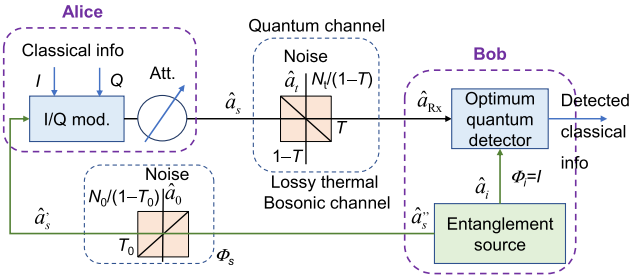

FIGURE 2. Illustrating the entanglement assisted classical communication system model with imperfect pre-shared entanglement distribution. I/Q mod: I/Q modulator, Att.: attenuator (it is optional).

in an optimum quantum receiver. In all papers on entanglement assisted classical communication, such as [4]–[8], it is assumed that the pre-shared entanglement is distributed perfectly, except for the attenuation effect, which is not possible in practice. We consider more realistic scenario as shown in Fig. 2, where the pre-shared entanglement is distributed with the help of two channels: signal channel, denoted by Φ_s, and the idler channel, denoted by Φ_i. We assume that entangled source is located on Bob's side, so that the idler channel is perfect, that is $\Phi_i = I$, where I is the identity operator. On the other hand, the signal channel Φ_s is modelled as a single-mode thermal lossy Bosonic channel, described by the Heisenberg evolution $\hat{a}_s' = \sqrt{T_0}\hat{a}_s'' + \sqrt{1-T_0}\hat{a}_0$, where T_0 is the transmissivity of Bob-to-Alice entanglement distribution channel Φ_s, while $\hat{a}_0$ is a thermal state with the mean photon number being $N_0/(1-T_0)$. The main (Alice-to-Bob) channel is also modelled by the single-mode thermal lossy Bosonic channel, described by the Heisenberg evolution $\hat{a}_{Rx} = \sqrt{T}\hat{a}_s + \sqrt{1-T}\hat{a}_t$, where $T \leq T_0$ is the transmissivity of the main channel, while $\hat{a}_t$ is a thermal state with the mean photon number being $N_t/(1-T)$, $N_t \geq N_0$. Clearly the main channel can also be interpreted as a zero-mean additive white Gaussian noise (AWGN) channel with power-spectral density of N_t and attenuation coefficient of T. Alice modulates the signal mode $\hat{a}_s'$ with the help of an I/Q modulator, as shown in Fig. 2, by effectively performing the following transformation $\hat{a}_s = s\hat{a}_s'$, where $s = s_I + js_Q$ is the transmitted signal constellation point. The coordinates for Gaussian modulation s_I and s_Q are generated from a zero-mean 2-D Gaussian distribution in the digital domain, a digital-to- analog converter (DAC) is used to represent the samples, which are further used as RF inputs of the I/Q modulator. The Gaussian samples are properly scaled to account for I/Q modulator insertion loss such that average number of transmitted signal photons per mode is equal to $N_s = \left\langle \hat{a}_s^\dagger \hat{a}_s \right\rangle = \left\langle s^\dagger s \, (\hat{a}_s')^\dagger \hat{a}_s' \right\rangle$. Alternatively, instead of I/Q modulator, the polar modulator can be used [17]. In related paper [7], in their communication system assisted by two-mode squeezed states authors use an I/Q modulator but in different context, to introduce the displacement to the signal photon state.

From Holevo's papers [4],[5] we know that the quantum limit of classical capacity is given by:

$$C_{\text{without EA}} = g\left(TN_s + N_t\right) - g\left(N_t\right), \tag{1}$$

which is also known as the *Holevo capacity*, wherein $g(x) = (x+1)\log_2(x+1) - x\log_2 x$. Given that according to the uncertainty principle both in-phase and quadrature components of a Gaussian state cannot be simultaneously measured with the complete precision, for homodyne detection the information is encoded on a single quadrature so that the average number of received photon is $4TN_s$, while the average number of noise photons is $2N_t+1$, and the corresponding classical capacity for homodyne detection is $C_{\text{hom}} = 0.5\log_2[1+4TN_s/(2N_t+1)]$. On the other hand, in heterodyne detection both quadratures are used so that the average number of received signal photons will be 0.5*0.5*4 $TN_s = TN_s$ (one-half comes from splitting to two quadratures and second half from heterodyne splitting), while the average number of noise photons per quadrature is $(2N_t+1)/2+1/2 = N_t+1$. The corresponding heterodyne channel capacity will be $C_{\text{het}} = \log_2[1+TN_s/(N_t+1)]$. To achieve the channel capacity in classical case we need to use the Gaussian modulation (GM) by generating samples from two Gaussian sources and with the help of an arbitrary waveform generator (AWG) impose them on the optical carrier by using an I/Q modulator. To achieve the Holevo capacity we need to use the Gaussian state. For instance the coherent state with GM can achieve the Holevo capacity.

The TMSV state, achieving the EA capacity according to [4], can be represented as:

$$\left|TMSV(N_s)\right\rangle_{s,i} = \frac{1}{\sqrt{N_s+1}}\sum_{n=0}^{\infty}\left(\frac{N_s}{N_s+1}\right)^{n/2}|n\rangle_s|n\rangle_i \quad (2)$$

and has the covariance matrix:

$$\mathbf{\Sigma}_{TMSV} = \begin{bmatrix} (2N_s+1)\mathbf{1} & 2\sqrt{N_s(N_s+1)}\mathbf{Z} \\ 2\sqrt{N_s(N_s+1)}\mathbf{Z} & (2N_s+1)\mathbf{1} \end{bmatrix}, \quad (3)$$

where $\mathbf{1}$ is the identity matrix and $\mathbf{Z} = \text{diag}(1,-1)$ is the Pauli Z-matrix.

Given that the action of the beam splitter (BS) can be represented by $BS(\tau) = \begin{bmatrix} \sqrt{\tau}\mathbf{1} & \sqrt{1-\tau}\mathbf{1} \\ -\sqrt{1-\tau}\mathbf{1} & \sqrt{\tau}\mathbf{1} \end{bmatrix}$, in order to determine the covariance matrix after the beam splitter in entanglement distribution channel (see Fig. 2) we need to apply the sympletic operation [1],[3] by

$$BS_c(T_0) = \mathbf{1} \oplus BS(T_0) = \begin{bmatrix} \mathbf{1} & \mathbf{0} & \mathbf{0} \\ \mathbf{0} & \sqrt{T_0}\mathbf{1} & \sqrt{1-T_0}\mathbf{1} \\ \mathbf{0} & -\sqrt{1-T_0}\mathbf{1} & \sqrt{T_0}\mathbf{1} \end{bmatrix} \quad (4)$$

on the input covariance matrix $\mathbf{\Sigma}_{TMSV}$ to obtain:

$$\mathbf{\Sigma}' = BS_c(T_0)\begin{bmatrix} \mathbf{\Sigma}_{TMSV} & \mathbf{0} \\ \mathbf{0} & \sigma'^2\mathbf{1} \end{bmatrix}[BS_c(T_0)]^T, \quad (5)$$

where the variance of thermal state is $N_0/(1-T_0)$ thermal photons. By keeping Alice and Bob submatrices we obtain:

$$\mathbf{\Sigma}'_{AB} = \begin{bmatrix} (2N_s+1)\mathbf{1} & 2\sqrt{T_0N_s(N_s+1)}\mathbf{Z} \\ 2\sqrt{T_0N_s(N_s+1)}\mathbf{Z} & (2N_s'+1)\mathbf{1} \end{bmatrix}, \quad (6)$$

where $N_s' = N_sT_0 + N_0$. By repeating the similar procedure for lossy and noisy Bosonic main channel we obtain the following covariance matrix for the zero-mean Gaussian state $\hat{\rho}_{Rx,i}$:

$$\mathbf{\Sigma}_{AB} = \begin{bmatrix} (2N_s+1)\mathbf{1} & 2\sqrt{T_0TN_s(N_s+1)}\mathbf{Z} \\ 2\sqrt{T_0TN_s(N_s+1)}\mathbf{Z} & (2N_s'+1)\mathbf{1} \end{bmatrix}, \quad (7)$$

where $N_s' = (N_sT_0+N_0)T + N_t$. Clearly, this covariance matrix has the standard form [12]–[16] $\mathbf{\Sigma} = \begin{bmatrix} a\mathbf{1} & \mathbf{C} \\ \mathbf{C} & b\mathbf{1} \end{bmatrix}$ with $a = 2N_s+1$, $b = 2N_s'+1$, $\mathbf{C} = c\mathbf{Z}$, $c = 2\sqrt{T_0TN_s(N_s+1)}$, and the symplectic eigenvalues are given by:

$$\begin{aligned} \nu_{\mp} &= \left[\sqrt{(a+b)^2-4c^2} \mp (b-a)\right]/2 \\ &= \sqrt{(N_s+N_s'+1)^2 - 4T_0TN_s(N_s+1)} \mp (N_s'-N_s). \end{aligned} \quad (8)$$

The corresponding expression for the entanglement assisted channel capacity is now simply:

$$C_{EA} = g(N_s) + g(N_s') - \left[g\left(\frac{\nu_+-1}{2}\right) + g\left(\frac{\nu_--1}{2}\right)\right]. \quad (9)$$

Here we propose to use TMSV state and modulate the signal photon by the zero-mean GM as illustrated in Fig. 2, by effectively mapping $\hat{a}_s' \to \hat{a}_s = s\hat{a}_s'$, where $s = s_I + js_Q$ is the transmitted signal constellation point with s_I and s_Q being generated from the 2-D zero-mean circular Gaussian noise source. The variance of 2-D Gaussian distribution is properly chosen such that the average number of transmitted signal photons is $\left\langle s^\dagger s\,(\hat{a}_s')^\dagger\hat{a}_s'\right\rangle = N_s$ so that the covariance matrix (7) is not affected. In incoming section, we compare the EA classical capacity against both (homodyne and heterodyne) classical and Holevo capacities.

III. ENTANGLEMENT ASSISTED COMMUNICATION VS. CLASSICAL OPTICAL COMMUNICATION

When the pre-shared entanglement can be perfectly distributed, as shown in Fig. 3, the EA capacity can indeed significantly outperform the Holevo capacity in very noisy regime $N_s \ll N_t$. When Alice employs the AWG to perform the GM of the signal photon, she is limited by the finite (l,k) precision (l: number of integer bits plus sign bit, k: number of decimal bits), and there is the limit for the lowest possible N_s. To solve for this problem we can scale the (I,Q) constellation point with a positive number and then apply an attenuator after the I/Q modulator. This scaling number is N_s-dependent. On such a way the (1,5) precision is sufficient to achieve the EA classical capacity. Notice that in these calculations we assume that the optimum quantum receiver is used.

For the realistic scenario, when the pre-shared entanglement is distributed over lossy thermal Bosonic channel, as shown in Fig. 4 the EA capacity improvement over both Holevo and classical capacities get significantly reduced. The Holevo capacity is identical to the homodyne capacity, while the heterodyne capacity is a little bit worse. When the entanglement distribution channel is identical to the communication channel the EA capacity is actually lower than the Holevo/homodyne capacity. When transmissivity of

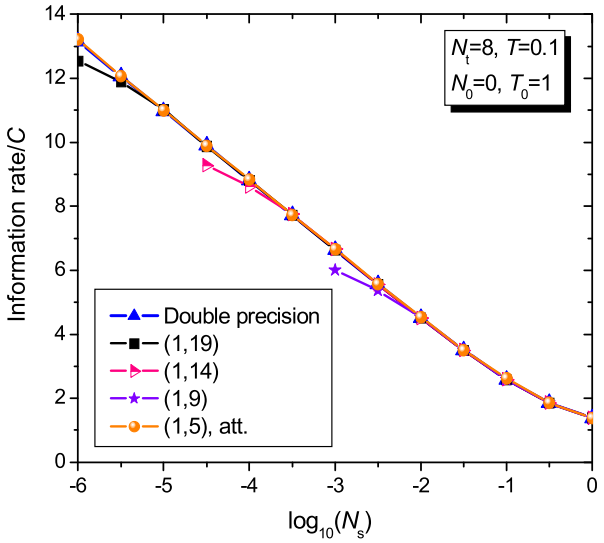

FIGURE 3. The normalized information rate vs. average number of signal photons N_S assuming that the pre-shared entanglement is perfectly distributed ($T_0 = 1$, $N_0 = 0$) and assuming that the optimum quantum receiver is used. The main channel transmissivity is set to $T = 0.1$ and the number of thermal photons to $N_t = 8$.

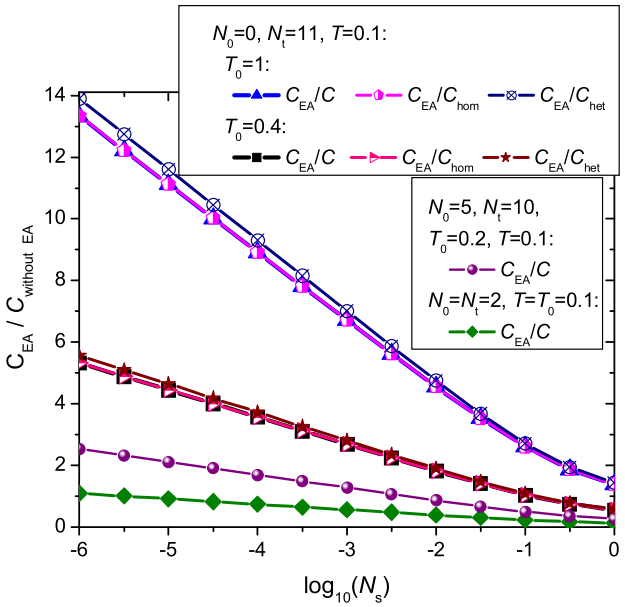

FIGURE 4. The improvement in capacity by entanglement assistance for imperfect pre-shared entanglement distribution.

entanglement distribution channel is higher than the transmissivity of the main (communication) channel, while at the same time is less noisy then the improvement of EA capacity over homodyne capacity is moderate to small (depending on actual value of the average number of signal photons). This particular case is applicable to Fig. 1(a), where the satellite links are used to distribute the pre-shared entanglement, while the free-space optical link with horizontal atmospheric turbulence for transmission of classical information. Namely, in the satellite-to-ground link turbulence is much weaker than the turbulence in horizontal links.

To see the actual improvement, expressed in bits/s/Hz, for this case we provide in Fig. 5 the plots for EA, Holevo,

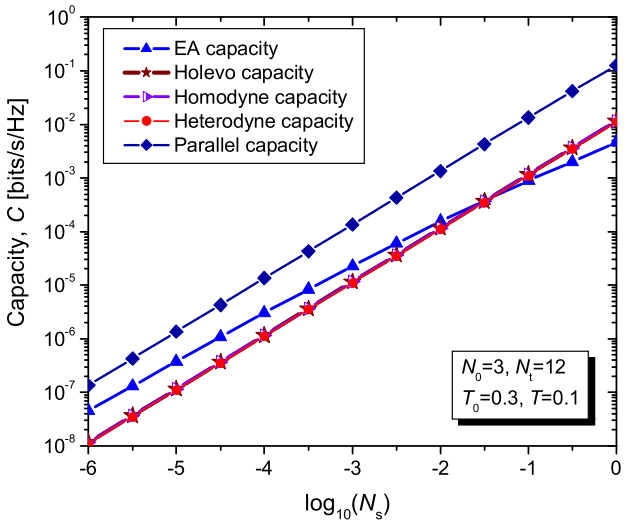

FIGURE 5. EA capacity vs. classical capacity when both main and entanglement distribution channels are noisy.

homodyne, and heterodyne capacities assuming that $N_0 = 3$, $N_t = 12$, $T_0 = 0.3$, and $T = 0.1$. For $N_s = 10^{-6}$, even though that the EA capacity is 3.9 times higher than homodyne capacity, the actual value of EA capacity is only $4.52 \cdot 10^{-8}$ bits/s/Hz. For average number of signal photons N_s between 0.01 and 0.1 the EA capacity performs comparable to the homodyne capacity, while for $N_s > 0.1$, the homodyne capacity outperforms the EA capacity.

In EA communication the entangled pair of photons is used, the signal photon for classical information transmission and the idler photon for entanglement assistance. In classical communication, only the main channel is used, and someone may speculate that this not a fair comparison. So naturally arises the question, what if we use the idler (auxiliary) channel for classical transmission instead? Overall classical capacity will be then addition of capacities of main and axillary channels, which is also shown in Fig. 5 as parallel capacity, which clearly outperforms EA capacity for all N_s values.

IV. ENTANGLEMENT ASSISTED COMMUNICATION OVER FSO LINKS

The beam propagation over FSO links is affected by various effects including the diffraction, atmospheric turbulence, and Mie scattering effects. The attenuation due to diffraction and scattering effects can be modelled by the transmissivity $T \in (0, 1]$ in the main (Alice-to-Bob) channel (see Fig. 2), while atmospheric turbulence is caused by variations in the refractive index of the transmission medium due to spatial variations in temperature and pressure (related to the wind and solar heating [17], [18]).

The atmospheric turbulence can be modelled as the multiplicative noise, described by the following probability density function of irradiance I [17], [18]:

$$f(I) = \frac{2(\alpha\beta)^{\frac{\alpha+\beta}{2}}}{\Gamma(\alpha)\Gamma(\beta)} I^{\frac{\alpha+\beta}{2}-1} K_{\alpha-\beta}\left(2\sqrt{\alpha\beta I}\right), \quad (10)$$

where α and β are the atmospheric turbulence parameters which for zero inner scale are defined, respectively, as [17], [18]:

$$\alpha = \left\{ \exp\left[\frac{0.49\sigma_R^2}{\left(1+1.11\sigma_R^{12/5}\right)^{7/6}} \right] - 1 \right\}^{-1}, \quad \beta = \left\{ \exp\left[\frac{0.51\sigma_R^2}{\left(1+0.69\sigma_R^{12/5}\right)^{5/6}} \right] - 1 \right\}^{-1}, \tag{11}$$

wherein σ_R^2 denotes the Rytov variance, defined as:

$$\sigma_R^2 = 1.23\, C_n^2\, k^{7/6} L^{11/6}. \tag{12}$$

In (12) C_n^2 denotes the refractive structure parameter, k is the wave number ($k = 2\pi/\lambda$, with λ being the wavelength), and L denotes the propagation distance. The Rytov variance can serve an indicator of the strength of the atmospheric turbulence effects. When $\sigma_R^2 < 1$ we say that turbulence is weak, for $\sigma_R^2 \approx 1$ we say that turbulence is medium, the strong turbulence fluctuations are specified with $\sigma_R^2 > 1$, while the saturation regime is defined by $\sigma_R^2 \to \infty$ [17], [18].

The covariance matrix of the zero-mean Gaussian state $\hat{\rho}_{Rx,i}$ in the presence of turbulence can be represented by:

$$\mathbf{\Sigma}_{AB}(I) = \begin{bmatrix} (2N_s+1)\,\mathbf{1} & 2\sqrt{IT_0TN_s(N_s+1)}\mathbf{Z} \\ 2\sqrt{IT_0TN_s(N_s+1)}\mathbf{Z} & \left(2N_s'+1\right)\mathbf{1} \end{bmatrix}, \tag{13}$$

where $N_s' = (N_sT_0 + N_0)\,TI + N_t$. The corresponding channel capacities are now functions of irradiance I, that is $C(I)$ is now a random variable. For instance the EA capacity in the presence of turbulence is evaluated by:

$$C_{EA} = \int_0^\infty C_{EA}(I) f(I)\, dI. \tag{14}$$

To evaluate the *ergodic* capacities we perform the Monte Carlo integration. For every channel use we generate a different realization of irradiance form the gamma-gamma distribution, calculate channel capacities for each realization $C(I)$, and average them out by $C = [\sum C(I)]/L$, where L is the number of realizations. Atmospheric turbulence also introduces the random phase shift, and we assume that a referent classical beam at sufficiently different wavelength is used to estimate and compensate for random phased shift and also to synchronize the transmitter and receiver. This approach has been applied to both classical and EA communications. To compensate for intensity fluctuations someone may use the adaptive optics (AO) approaches [20], [21]. However, the AO can fully compensate the turbulence effects only in weak turbulence regime.

Let us now study how the improvement in EA capacity over classical capacities is affected by atmospheric turbulence effects. For Rytov standard deviation $\sigma_R = 4$ (Rytov variance $\sigma_R^2 = 16$), corresponding to strong turbulence in the main channel, in Fig. 6(a) we summarize the EA capacity improvement over Holevo capacity for imperfect distribution of entanglement, assuming that entanglement distribution

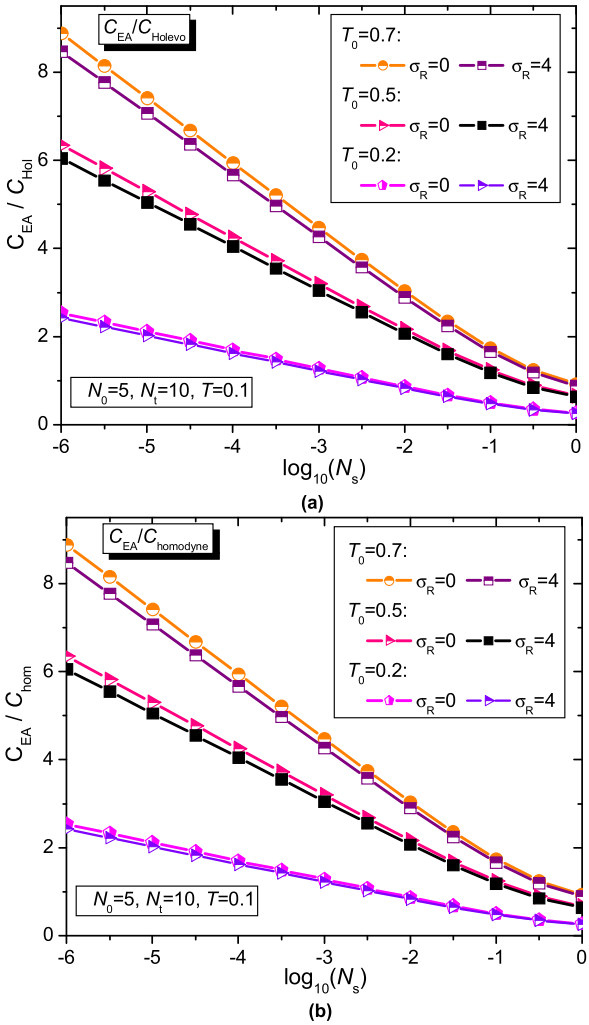

FIGURE 6. The improvement in capacity by entanglement assistance for imperfect pre-shared entanglement distribution in the presence of atmospheric turbulence in main channel: (a) C_{EA}/C_{Hol} and (b) C_{EA}/C_{hom}.

channel is modeled as noisy Bosonic channel with $N_0 = 5$. In addition to turbulence, we assume that the main channel is also affected by diffraction and scattering effects modeled by transmissivity $T = 0.1$. We also assume that in the main channel there exists the background noise with $N_t = 10$. This situation corresponds to Fig. 1(b), where entanglement is distributed over the fiber-based quantum network, and the main channel is an FSO link. Clearly, there is certain degradation in EA capacity compared to the Holevo capacity, in particular when the transmissivity of the entanglement distribution channel is $T_0 \geq 0.5$. On the other hand, in Fig. 6(b) we summarize the EA capacity improvement over homodyne capacity under the same assumptions as in Fig. 6(a). Clearly, the trend is similar as in Fig. 6(a).

To see actual improvement in EA capacity over Holevo and classical capacities for strong turbulence, in Fig. 7 we plot capacities vs. average number of signal photons N_s assuming that entanglement distributed channel is noisy and lossy Bosonic ($N_0 = 2$, $T_0 = 0.5$), while the main channel is affected by strong turbulence ($\sigma_R = 4$), in addition to scattering/diffraction effects ($T = 0.1$) and noise ($N_t = 12$). As long

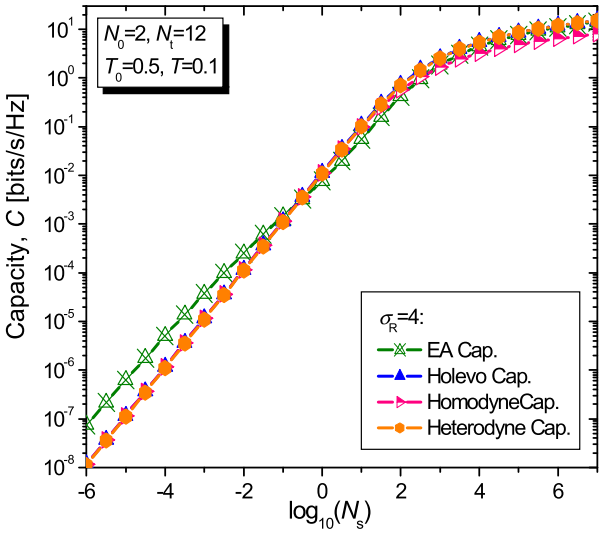

FIGURE 7. **EA capacity vs. classical capacity when main channel is affected by turbulence while entanglement distribution channel is noisy.**

as $N_s < 0.1$, the EA capacity outperforms classical capacities. Holevo and heterodyne capacities are almost identical, while the heterodyne capacity is higher than homodyne capacity for $N_s > 100$.

V. CONCLUDING REMARKS

When the pre-shared entanglement is imperfect, the EA communication in highly noisy environment can be better than classical communication with homodyne detection only if the entanglement distribution channel is less noisy than the main channel and has better transmissivity than the main channel. When both communication and entanglement distribution channels are not used for EA communication but for classical communication instead than the overall classical capacity is always higher than the EA capacity. In the presence of strong atmospheric turbulence in the main channel, the improvement of EA capacity over classical capacity is lower compared to the case without turbulence, but the degradation is not significant.

Even though that the optimum encoding, achieving the EA channel capacity, has been known for decades [4], [5], the design of optimum quantum receiver appears to be still an open problem, although some progress has been made recently [8]. For instance, authors in [8] proposed to use the multiple sections of the feed-forward (FF)-sum-frequency generation (SFG) receiver, initially proposed to detect the target in highly noisy environment [19]. Unfortunately, the complexity of this scheme is too high and has not been experimentally demonstrated yet.

REFERENCES

[1] I. B. Djordjevic, *Physical-Layer Security and Quantum Key Distribution*. Cham, Switzerland: Springer, 2019.

[2] G. Cariolaro, *Quantum Communications*. Cham, Switzerland: Springer, 2015.

[3] I. B. Djordjevic, *Quantum Information Processing, Quantum Computing, and Quantum Error Correction: An Engineering Approach*, 2nd ed. New York, NY, USA: Academic, 2021.

[4] A. Holevo and R. Werner, "Evaluating capacities of bosonic Gaussian channels," *Phys. Rev. A, Gen. Phys.*, vol. 63, no. 3, Feb. 2001, Art. no. 032312.

[5] A. S. Holevo, "On entanglement-assisted classical capacity," *J. Math. Phys.*, vol. 43, no. 9, pp. 4326–4333, 2002.

[6] C. H. Bennett, P. W. Shor, J. A. Smolin, and A. V. Thapliyal, "Entanglement-assisted capacity of a quantum channel and the reverse Shannon theorem," *IEEE Trans. Inf. Theory*, vol. 48, no. 10, pp. 2637–2655, Oct. 2002.

[7] M. Sohma and O. Hirota, "Capacity of a channel assisted by two-mode squeezed states," *Phys. Rev. A, Gen. Phys.*, vol. 68, no. 2, Aug. 2003, Art. no. 022303.

[8] H. Shi, Z. Zhang, and Q. Zhuang, "Practical route to entanglement-assisted communication over noisy bosonic channels," *Phys. Rev. Appl.*, vol. 13, no. 3, Mar. 2020, Art. no. 034029.

[9] R. Van Meter and S. J. Devitt, "The path to scalable distributed quantum computing," *Computer*, vol. 49, no. 9, pp. 31–42, Sep. 2016.

[10] Z. Zhang and Q. Zhuang, "Distributed quantum sensing," 2020, *arXiv:2010.14744*. [Online]. Available: http://arxiv.org/abs/2010.14744

[11] A. M. Childs, "Secure assisted quantum computation," *Quantum Inf. Comput.*, vol. 5, no. 6, pp. 456–466, 2005.

[12] R. Simon, "Peres–Horodecki separability criterion for continuous variable systems," *Phys. Rev. Lett.*, vol. 84, no. 12, p. 2726, 2000.

[13] L.-M. Duan, G. Giedke, J. I. Cirac, and P. Zoller, "Inseparability criterion for continuous variable systems," *Phys. Rev. Lett.*, vol. 84, no. 12, p. 2722, 2000.

[14] A. Serafini, "Multimode uncertainty relations and separability of continuous variable states," *Phys. Rev. Lett.*, vol. 96, no. 11, Mar. 2006, Art. no. 110402.

[15] S. Pirandola, A. Serafini, and S. Lloyd, "Correlation matrices of two-mode bosonic systems," *Phys. Rev. A, Gen. Phys.*, vol. 79, no. 5, May 2009, Art. no. 052327.

[16] C. Weedbrook, S. Pirandola, R. García-Patrón, N. J. Cerf, T. C. Ralph, J. H. Shapiro, and S. Lloyd, "Gaussian quantum information," *Rev. Mod. Phys.*, vol. 84, no. 2, pp. 621–669, 2012.

[17] I. B. Djordjevic, *Advanced Optical and Wireless Communications Systems*. Cham, Switzerland: Springer, 2018.

[18] L. C. Andrews and R. L. Philips, *Laser Beam Propagation Through Random Media*. Bellingham, WA, USA: SPIE, 2005.

[19] Q. Zhuang, Z. Zhang, and J. H. Shapiro, "Optimum mixed-state discrimination for noisy entanglement-enhanced sensing," *Phys. Rev. Lett.*, vol. 118, no. 4, Jan. 2017, Art. no. 040801.

[20] V. Nafria, X. Han, and I. B. Djordjevic, "Improving free-space optical communication with adaptive optics for higher order modulation," *Proc. SPIE*, vol. 11509, Aug. 2020, Art. no. 115090K.

[21] V. Nafria, C. Cui, I. B. Djordjevic, and Z. Zhang, "Adaptive-optics enhanced distribution of entangled photons over turbulent free-space optical channels," in *Proc. CLEO*, 2021, May 2021.

IVAN B. DJORDJEVIC (Fellow, IEEE) received the Ph.D. degree from the University of Nis, Yugoslavia, in 1999.

He is currently a Professor of electrical and computer engineering and optical sciences with the University of Arizona; the Director of the Optical Communications Systems Laboratory (OCSL) and Quantum Communications (QuCom) Laboratory; and the Co-Director of the Signal Processing and Coding Laboratory. Prior to joining the University of Arizona, he held appointments with the University of Bristol; the University of the West of England, U.K.; Tyco Telecommunications, USA; the National Technical University of Athens, Greece; and State Telecommunication Company, Yugoslavia. He has authored or coauthored eight books, more than 540 journal and conference publications, and holds 54 U.S. patents.

Dr. Djordjevic is also an OSA Fellow. Since 2016, he has been serving as an Associate Editor/a member of editorial board for *IOP Journal of Optics* and *Physical Communication Journal* (Elsevier). He also serves as an Area Editor/an Associate Editor/a member of editorial board for the journals, such as IEEE Communications Letters, OSA/IEEE Journal of Optical Communications and Networking, *Optical and Quantum Electronics*, and *Frequenz*.